

Cite this: *Dalton Trans.*, 2019, **48**, 15247

Two telomerase-targeting Pt(II) complexes of jatrorrhizine and berberine derivatives induce apoptosis in human bladder tumor cells†

Qi-Pin Qin, *^{a,b} Zhen-Feng Wang,^a Xiao-Ling Huang,^a Ming-Xiong Tan, *^a Zhi-Hui Luo,*^a Shu-Long Wang,^a Bi-Qun Zou *^{b,c} and Hong Liang*^b

Two novel Pt(II) complexes, [Pt(B-TFA)Cl]Cl (**Pt1**) and [Pt(J-TFA)Cl]Cl (**Pt2**) with jatrorrhizine and berberine derivatives (**B-TFA** and **J-TFA**) were first prepared as desirable luminescent agents for cellular applications and potent telomerase inhibitors, which can induce bladder T-24 tumor cell apoptosis by targeting telomerase, together with induction of mitochondrial dysfunction, telomere DNA damage and cell-cycle arrest. Importantly, T-24 tumor inhibition rate (TIR) was 50.4% for **Pt2**, which was higher than that of **Pt1** (26.4%) and cisplatin (37.1%). Taken together, all the results indicated that jatrorrhizine and berberine derivatives **Pt1** and **Pt2** show low toxicity and could be novel Pt-based anti-cancer drug candidates.

Received 5th June 2019,
Accepted 24th September 2019

DOI: 10.1039/c9dt02381j

rsc.li/dalton

Introduction

Cisplatin and its derivatives have become the most widely used anti-cancer agents in the clinics.^{1,2} However, Pt-based agents can cause toxicity and resistance. Great efforts have been made in the design of the novel Pt(II/IV) anti-cancer compounds, which are more effective against typically Pt(II)-refractory tumour cells.^{3,4}

Up to now, metal complexes with a large number of natural products isolated from traditional Chinese medicines (TCMs), such as liriodenine, oxoglucine, plumbagin, matrine, oxoisoaporphine, coumarin and oxoaporphine, have been explored for their selective anti-tumor activities.^{5–7} More significantly, (ox) oisoaporphine Pt(II) and Ru(II) complexes have been reported as telomerase inhibitors targeting telomeric G-quadruplex DNA (G4 DNA), and exhibited high tumor inhibitory effects *in vivo* and *in vitro*.⁷ Telomerase is over-expressed in 85–90% of cancer cells but has undetectable activity in the normal cell line,^{7,8} thus its specific expression in tumor cells has

prompted the design of next-generation TCMs telomerase-targeting Pt(II) anti-cancer complexes.

Berberine (**1**) and jatrorrhizine (**7**) are the major bioactive alkaloids isolated from *Tinospora capillipes* Gagnep.⁹ They are important compounds because of their wide range of pharmacological activities including antifungal, anti-tumor, and anti-bacterial activities.⁹ However, no jatrorrhizine and berberine metal complexes have been reported. Herein, we report the preparation and exploration of the *in vitro* and *in vivo* anti-cancer mechanisms of Pt(II) complexes with jatrorrhizine and berberine derivatives.

Results and discussion

Synthesis and characterization of jatrorrhizine and berberine derivatives and their complexes **Pt1** and **Pt2**

Berberine (**1**) and jatrorrhizine (**7**) were the major bioactive alkaloids isolated from *Tinospora capillipes* Gagnep.⁹ In addition, the structures of two novel Pt(II) complexes with jatrorrhizine and berberine derivatives [Pt(B-TFA)Cl]Cl (**Pt1**) (B-TFA = trifluoroacetic acid 9-[9-(bis-pyridin-2-ylmethyl-amino)-nonyloxy]-10-methoxy-5,6-dihydro-[1,3]dioxolo[4,5-g]isoquino[3,2-a]isoquinolin-7-ylum; TFA = trifluoroacetic acid) and [Pt(J-TFA)Cl]Cl (**Pt2**) (J-TFA = trifluoroacetic acid 3-[9-(bis-pyridin-2-ylmethyl-amino)-nonyloxy]-2,9,10-trimethoxy-5,6-dihydroisoquino[3,2-a]isoquinolinylum) are presented in Fig. 1, Schemes S1 and S2.† The two jatrorrhizine and berberine derivatives, and their Pt(II) complexes **Pt1** and **Pt2** were first synthesized (Fig. 1, Schemes S1 and S2†), starting from berberine (**1**) and jatrorrhizine (**7**). In addition, the characterization

^aGuangxi Key Lab of Agricultural Resources Chemistry and Biotechnology, College of Chemistry and Food Science, Yulin Normal University, 1303 Jiaoyudong Road, Yulin 537000, PR China. E-mail: qpqin2018@126.com, mxtan2018@126.com, lzhuo_1980@163.com; Fax: +86-775-2623650; Tel: +86-775-2623650

^bState Key Laboratory for the Chemistry and Molecular Engineering of Medicinal Resources, School of Chemistry and Pharmacy, Guangxi Normal University, 15 Yucui Road, Guilin 541004, PR China. E-mail: hliang@mailbox.gxnu.edu.cn

^cDepartment of Chemistry, Guilin Normal College, 9 Feihu Road, Guilin 541001, China. E-mail: zoubiqun@163.com

† Electronic supplementary information (ESI) available: Experimental details and figures. See DOI: 10.1039/c9dt02381j

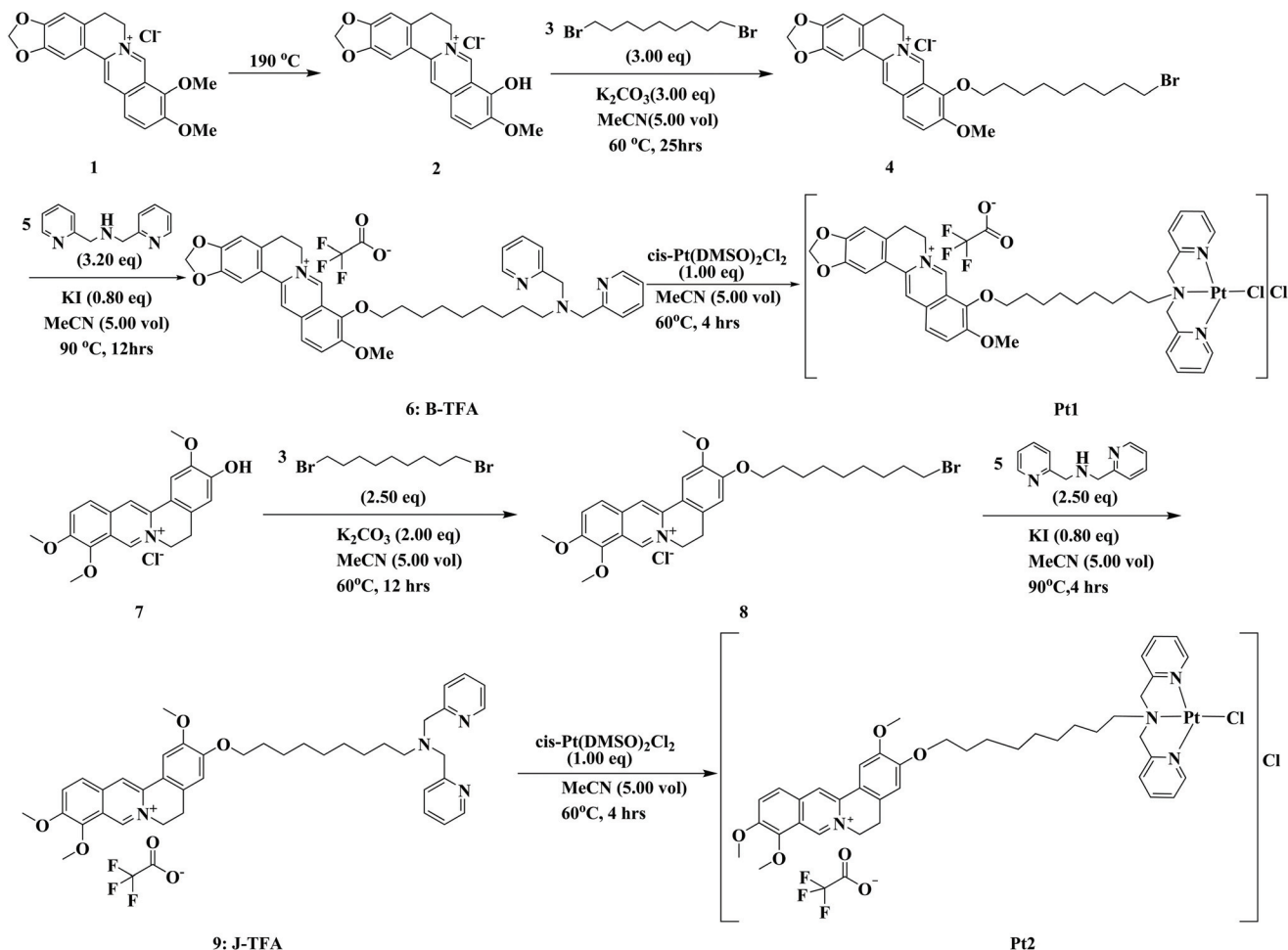


Fig. 1 Synthetic routes for the preparation of trifluoroacetic acid 9-[9-(bis-pyridin-2-ylmethyl-amino)-nonyloxy]-10-methoxy-5,6-dihydro-[1,3]dioxolo[4,5-g]isoquino[3,2-a]isoquinolin-7-ylum (B-TFA), trifluoroacetate 3-[9-(bis-pyridin-2-ylmethyl-amino)-nonyloxy]-2,9,10-trimethoxy-5,6-dihydro-isoquino[3,2-a]isoquinolinylum (J-TFA) and their Pt(II) complexes Pt1 and Pt2.

of Pt1 and Pt2 and their stability in Tris-HCl solution (pH = 7.35, 10.0 mM) are presented in Fig. S1–S24 (ESI[†]).

In vitro anti-cancer activity

Next, the cytotoxicity of Pt1 and Pt2 was assessed with MTT assay using human bladder T-24 tumor cells, cisplatin-resistant cancer SK-OV-3 cells (SK-OV-3/DDP), lung cancer A549 cells and hepatocyte normal HL-7702 cells. For comparison, the B-TFA, *cis*-Pt(DMSO)₂Cl₂ (PtD), (B-TFA + PtD), (J-TFA + PtD), TFA, J-TFA, and cisplatin were also treated under the same conditions (Table 1). Importantly, Pt1 and Pt2 has much lower IC₅₀ values (10.0 nM–15.2 μM) against the human bladder T-24 tumor cells, cisplatin-resistant cancer SK-OV-3 cells (SK-OV-3/DDP), and lung cancer A549 cells than the corresponding B-TFA and J-TFA ligands, *cis*-Pt(DMSO)₂Cl₂ (PtD), the mix (B-TFA + PtD) and (J-TFA + PtD) compounds, suggesting the synergistic effect in Pt1 and Pt2 after the berberine and jatrorrhizine B-TFA and J-TFA ligands as a functional group were coordinated to the Pt(II) metal, respectively. More significantly, Pt2 showed rapid uptake into cancer cells, and displayed

Table 1 IC₅₀ (μM) of Pt1 and Pt2 towards human cells

	T-24	SK-OV-3/DDP	A549	HL-7702
B-TFA	18.7 ± 0.3	>100	28.3 ± 1.4	>150
Pt1	0.1 ± 0.1	10.2 ± 0.7	15.2 ± 0.8	>150
J-TFA	13.2 ± 0.9	>100	18.6 ± 1.2	>150
Pt2	10.0 ± 0.2 nM	5.1 ± 1.5	9.3 ± 1.5	>150
PtD	>150	>150	>150	>150
B-TFA + PtD	17.3 ± 0.9	>100	28.1 ± 0.5	>150
J-TFA + PtD	13.0 ± 0.1	>100	18.4 ± 0.7	>150
TFA	75.3 ± 0.6	94.2 ± 1.5	81.1 ± 0.2	61.2 ± 0.5
Cisplatin	10.4 ± 1.2	65.3 ± 1.9	16.0 ± 1.1	17.3 ± 0.9

obvious cytotoxicity against human bladder cell line T-24 after treatment for 6.0 h, with an IC₅₀ value of 10.0 ± 0.2 nM, which was 1870.0, 10.0, 1320.0 and 1040.0 times lower than that of B-TFA, Pt1, J-TFA, and cisplatin, respectively. Remarkably, Pt1 and Pt2 showed low cytotoxicity (IC₅₀ > 150 μM) against normal HL-7702 cells. Importantly, jatrorrhizine derivatives complex Pt2 showed stronger antitumor activity (10.0 ± 0.2 nM) against bladder T-24 tumor cells than that of liriodenine,

oxoglucaine, plumbagin, matrine, oxoisoaporphine, coumarin and oxoaporphine metal complexes.^{5–7}

Cellular uptake

Table S1† shows that the cellular platinum(II) amount for **Pt2** was $(31.27 \pm 0.05 \text{ ng of Pt})$ per 10^6 cells, 1.4- and 4.1-times higher than that of **Pt1** ($(15.06 \pm 0.03 \text{ ng of Pt})$ per 10^6 cells), cisplatin ($(5.25 \pm 0.03 \text{ ng of Pt})$ per 10^6 cells), liriodenine, oxoglucaine, plumbagin, matrine, oxoisoaporphine, coumarin and oxoaporphine metal complexes,^{5–7} after treatment for 6 h. As expected, the distribution of **Pt2** (10.0 nM) in nuclear or mitochondria fraction was higher than those of **Pt1** (100.0 nM) and cisplatin (10.4 μM). Furthermore, confocal microscopy analysis indicated that **Pt1** (100.0 nM) and **Pt2** (10.0 nM) exhibited 525–530 nm emission in T-24 cancer cells under ambient conditions upon excitation at 490–495 nm (Fig. 2–4 and S25†), which acted as green-colored luminescent agents for cellular applications. These images also suggested that **Pt1** (100.0 nM) and **Pt2** (10.0 nM) could be effectively taken up by T-24 cancer cells and were mainly retained within the nuclear fraction and targeted 53BP1, TRF1 and TRF2 after 6.0 h of incubation (Fig. 2 and S25†).

Pt1 and Pt2 induced telomeres damage

Mammalian telomeres consist of TRF1 and TRF2 two telomere-specific proteins, which were closely associated with telomere dysfunction/damage, telomere length, telomere maintenance and telomere inhibition.^{7,10} Furthermore, 53BP1 has emerged as a key of DNA/telomere damage response factors. In general, overexpression of 53BP1, TRF1 and TRF2 (emitted skyblue fluorescence in the merge) in cancer cells, suggesting that these Pt compounds can significantly induce telomeres damage (TRF1 and TRF2) and DNA damage (53BP1).^{7,10} To investigate the effects of **Pt1** (100.0 nM) and **Pt2** (10.0 nM) on telomere dysfunction, immunofluorescence assay of the levels

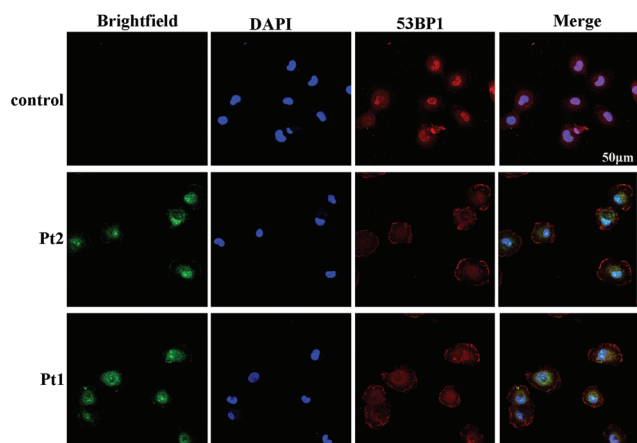


Fig. 2 **Pt1** (100.0 nM) and **Pt2** (10.0 nM) induced telomere dysfunction in T-24 cells. The T-24 cells were incubated with **Pt1** (100.0 nM) and **Pt2** (10.0 nM) at 37 °C for 6 h, and then processed for 53BP1 (red) and the nuclei were stained with DAPI (blue). Excitation wavelength (λ_{ex}) of **Pt1** and **Pt2**: 490–495 nm; emission filters (λ_{em}): 525–530 nm.

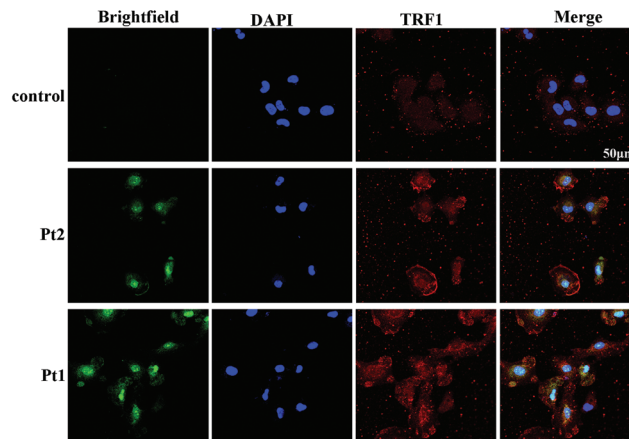


Fig. 3 **Pt1** (100.0 nM) and **Pt2** (10.0 nM) induced telomere dysfunction in T-24 cells. The T-24 cells were incubated with **Pt1** (100.0 nM) and **Pt2** (10.0 nM) at 37 °C for 6 h, and then processed for TRF1 (red) and the nuclei were stained with DAPI (blue). Excitation wavelength (λ_{ex}) of **Pt1** and **Pt2**: 490–495 nm; emission filters (λ_{em}): 525–530 nm.

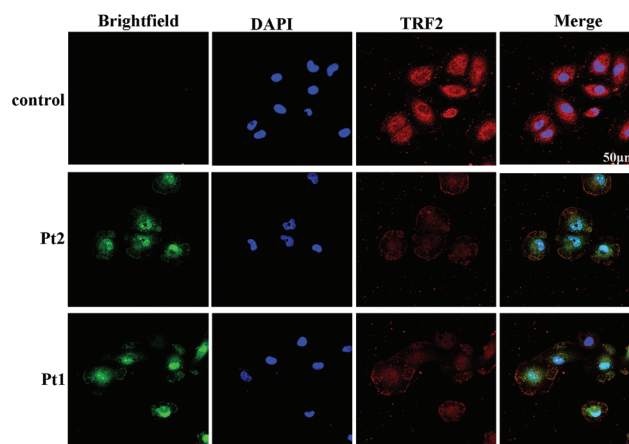


Fig. 4 **Pt1** (100.0 nM) and **Pt2** (10.0 nM) induced telomere dysfunction in T-24 cells. The T-24 cells were incubated with **Pt1** (100.0 nM) and **Pt2** (10.0 nM) at 37 °C for 6 h, and then processed for TRF2 (red) and the nuclei were stained with DAPI (blue). Excitation wavelength (λ_{ex}) of **Pt1** and **Pt2**: 490–495 nm; emission filters (λ_{em}): 525–530 nm.

of telomere-related proteins in T-24 cells were performed. As shown in Fig. 2–4 and S25,† the levels of TRF1, 53BP1 and TRF2 expression were more remarkably increased after treated with **Pt2** (10.0 nM) than that of **Pt1** (100.0 nM), and these bladder T-24 tumor cells showed typical DNA damage features, such as nuclear shrinkage (brightly stained), suggesting **Pt1** (100.0 nM) and **Pt2** (10.0 nM) can induce TRF1- and TRF2-telomeres damage.^{7,10}

Telomerase inhibition

Recently, c-myc, hTERT and telomerase inhibitory activity are considered as key factors in cancer cell apoptosis.^{7,11} Because **Pt1** (100.0 nM) and **Pt2** (10.0 nM) were accumulated in nuclear fraction (Table S1†), thus TRAP-silver staining assay and

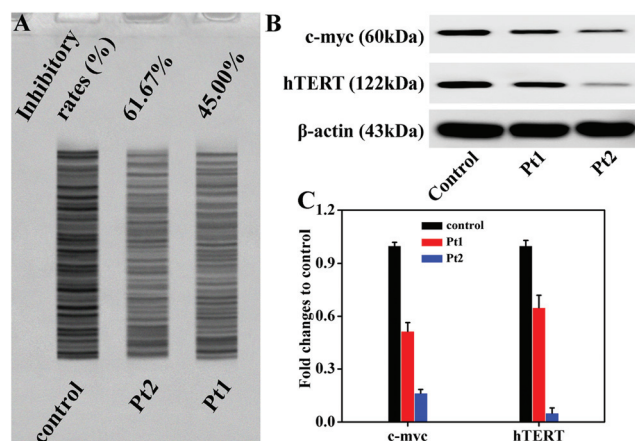


Fig. 5 Pt1 (100.0 nM) and Pt2 (10.0 nM) inhibited the expressions of telomerase (A) and related proteins (B and C) in bladder T-24 tumor cells after treatment for 6 h.

western blot assay were carried out. As shown in Fig. 5B and C, Pt2 (10.0 nM) with J-TFA ligand exhibited stronger c-myc and hTERT inhibitory activity in T-24 cells than Pt1 with B-TFA ligand, which was 3.1 and 13.0 times lower than that of Pt1, respectively. Further, as shown in the Fig. 5A and S26,† the telomerase inhibitory ratio (TIR) induced by jatrorrhizine complex Pt2 (10.0 nM) was 61.67% in bladder T-24 tumor cells that was higher than berberine complex Pt1 (100.0 nM, TIR = 45.00%), the corresponding ligands B-TFA (18.7 μM, TIR = 4.50%), J-TFA (13.2 μM, TIR = 31.83%) and previously reported TCMs metal complexes,^{5–7} respectively. These results indicated that Pt1 (100.0 nM) and Pt2 (10.0 nM) induced telomerase activity in T-24 cells was significantly correlated with the down-regulation of hTERT and c-myc levels.^{7,11}

Cell-cycle regulation

Telomerase inhibition also plays a key role in cell-cycle regulation.^{11,12} After Pt1 (100.0 nM) and Pt2 (10.0 nM) treatment, the population of cells at the G0/G1 phase was significantly increased to 52.68% and 54.59%, respectively, comparing with the 41.47% of control. In the meantime, the populations in the S and G2/M phases gradually decreased (Fig. 6 and S27†). G1 phase block and changes of cyclin D1-CDK2 complex were observed in Pt1 and Pt2 treated cells (Fig. 6, 7, S27 and S28†), which were more profound than the previously reported complexes.^{7,10}

Mitochondrial dysfunction

In addition, mitochondrial dysfunction activated by DNA damage can induce apoptosis of cancer cells.^{12,13} We showed that Pt1 (100.0 nM) and Pt2 (10.0 nM) were accumulated in mitochondrial fraction (Table S1†) and induced TRF1- and TRF2-telomeres damage (Fig. 2–4 and S25†). Fig. 7, S28 and S29† showed that Pt1 (100.0 nM) and Pt2 (10.0 nM) induced obvious up-regulation/down-regulation of cytochrome c, caspase-9, ROS (reactive oxygen species), caspase-3, bcl-2,

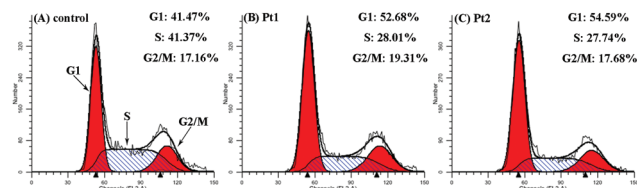


Fig. 6 Cell cycle arrest effect in T-24 cells after (B) Pt1 (100.0 nM) and (C) Pt2 (10.0 nM) treatment for 6.0 h, compared with control cells (A).

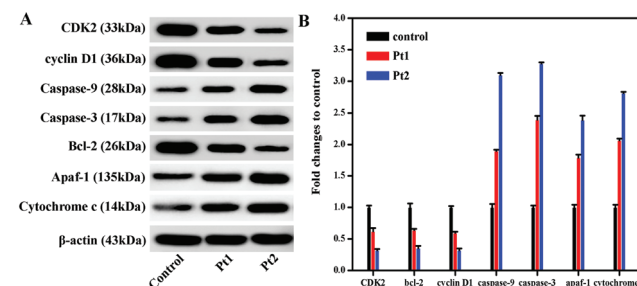


Fig. 7 (A) Western blot analysis to detect the levels of G1 phase- and apoptosis-related proteins after Pt1 (100.0 nM) and (C) Pt2 (10.0 nM) treatment for 6.0 h. (B) The whole cell extracts were prepared and analyzed by western blot analysis using antibodies against the related proteins.

[Ca²⁺] and apaf-1 expressions, especially for Pt2 (10.0 nM) treated cell. Moreover, Pt1 and Pt2 decreased the ΔΨ_m (mitochondrial membrane potential) level, and thereby activating the mitochondria-mediated apoptosis pathway.

Pt1 and Pt2 induced T-24 tumor cell apoptosis *in vitro* and *in vivo*

We next investigated whether Pt1 and Pt2 could induce T-24 tumor cell apoptosis *in vitro* and found that Pt2 (10.0 nM) indeed caused more apoptosis (Fig. 8A) in T-24 cells than Pt1

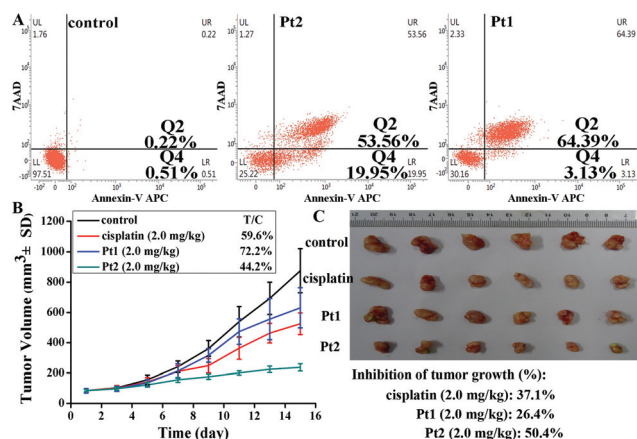


Fig. 8 Pt1 and Pt2 induced T-24 tumor cell apoptosis *in vitro* and *in vivo*. (A) Apoptosis of T-24 cells treated with Pt1 (100.0 nM) and Pt2 (10.0 nM) for 24 h. (B) The images and (C) changes of tumors or volumes after Pt2 (2.0 mg kg⁻¹ every 2 days (q2d)), Pt1 (2.0 mg kg⁻¹ q2d) and cisplatin (2.0 mg kg⁻¹ q2d) treated by intravenous injection.

(100.0 nM). Furthermore, the *in vivo* anti-cancer efficacy of **Pt2** (2.0 mg kg⁻¹ every 2 days (q2d)), **Pt1** (2.0 mg kg⁻¹ q2d) and cisplatin (2.0 mg kg⁻¹ q2d) on NCI-H460 xenograft was investigated. Tables S2–S4† and Fig. 8B, C show that the T-24 tumor inhibition rate (TIR) was 50.4% for **Pt2** (Tables S2–S4† and Fig. 8B, C), which was higher than that of **Pt1** (26.4%) and cisplatin (37.1%) and many previously reported Pt complexes.^{5–7,10,14,15} Remarkably, no damage and weight loss were observed for **Pt2** and **Pt1** treated mice (Tables S2–S4†), suggesting that the low systemic toxicity of Pt(II) complexes with jatrorrhizine and berberine derivatives.

Experimental materials and methods

Synthesis of B-TFA and J-TFA ligands

General procedure for preparation of compound 2. Berberine (**1**) and jatrorrhizine (**7**) were the major bioactive alkaloids isolated from *Tinospora capillipes* Gagnep.⁹ Berberine (**1**) (5.00 g, 13.4 mmol, 1.00 eq., HCl) was in three flask bottle. The mixture was under N₂ at 25 °C and warmed to 190 °C for 2 h. TLC (dichloromethane : methanol = 5 : 1, R_f = 0.55) indicated berberine (5.00 g, 13.4 mmol, 1.00 eq., HCl) was consumed completely and new spots formed. The 11-methoxy-21,22-dioxa-19-azoniapentacyclohenicosa-1,3(16),4(14),5(15),-6(19),10(17),11(18),12-octaen-18-ol (**2**) (3.75 g, 6.79 mmol, 50.7% yield) was obtained as a purple solid using LC-MS spectrometry. ESI-MS *m/z*: 322.1 [M – Cl]⁺ (Tris-HCl buffer solution containing 5% DMSO as solvent). Elemental analysis calcd (%) for C₁₉H₁₆ClNO₄: C 63.78, H 4.51, and N 3.91; found: C 63.76, H 4.54, and N 3.90.

General procedure for preparation of compound 4. Compound **2** (2.00 g, 6.20 mmol, 1.00 eq.) and 1,9-dibromononane (**3**) (5.32 g, 18.6 mmol, 3.00 eq.) were dissolved in MeCN (60.0 mL). K₂CO₃ (2.57 g, 18.6 mmol, 3.00 eq.) was added to the above mixture under N₂ at 25 °C and warmed to 60 °C for 24 h. TLC (dichloromethane : methanol = 10 : 1, R_f = 0.48) indicated compound **2** was remained, and one major new spot was detected. LC-MS indicated desired 27-(9-bromononyloxy)-20-methoxy-29,30-dioxa-28-azoniapentacyclohenicosa-1,3(25),4(23),5(24),6(28),19(26),20(27),21-octaene (**4**) (56.6% purity). The mixture was directly next step. ESI-MS *m/z*: 528.1 [M – Cl]⁺ (Tris-HCl buffer solution containing 5% DMSO as solvent). Elemental analysis calcd (%) for C₂₈H₃₃BrClNO₄: C 59.74, H 5.91, and N 2.49; found: C 59.73, H 5.93, and N 2.47.

General procedure for preparation of B-TFA. Compound **4** (4.00 g, 7.58 mmol, 1.00 eq.) and 1-(2-pyridyl)-N-(2-pyridylmethyl) methanamine (**5**) (4.84 g, 24.3 mmol, 3.20 eq.) were dissolved in MeCN (15.0 mL) at 25 °C. KI (1.01 g, 6.07 mmol, 0.80 eq.) was added to mixture to 90 °C for 12 h. The reaction mixture was filtered and concentrated under reduced pressure to remove MeCN (15.0 mL). The residue was diluted with DCM (15.0 mL × 3) and extracted with H₂O (30.0 mL). The combined organic layers were washed with H₂O (5.00 mL × 2), dried over Na₂SO₄, filtered and concentrated under reduced pressure to give a residue. The residue was purified by column chromatography

(SiO₂, dichloromethane : MeOH = 5 : 1). The residue was purified by prep-HPLC (column: Phenomenex luna C18 250 × 50 mm × 10 μm; mobile phase: [water(0.1%TFA)-ACN]; B%: 12%–42%, 20 min), and finally this target compound was obtained as a yellow oil. LC-MS, ¹H NMR and ¹⁹F NMR and ¹³C NMR desired 9-[(32-methoxy-44,45-dioxa-42-azoniapentacyclohenicosa-7,11(29)12(35),13-(36),14(38),32(39),33,37(42-octaen-39-yl)oxy]-N,N-bis(2-pyridylmethyl)nonan-1-amine (**B-TFA**) (1.25 g, 1.55 mmol, 7.13% yield). ¹H NMR (400 MHz, CHCl₃-d) δ 9.84 (s, 1H), 8.81 (d, *J* = 5.5 Hz, 2H), 8.26–8.20 (m, 2H), 8.20–8.16 (m, 1H), 7.87 (dd, *J* = 4.7, 8.3 Hz, 3H), 7.82–7.76 (m, 1H), 7.67 (t, *J* = 6.5 Hz, 2H), 7.36 (s, 1H), 6.85 (s, 1H), 6.11 (s, 2H), 5.01 (br t, *J* = 5.8 Hz, 2H), 4.42 (s, 4H), 4.36 (t, *J* = 6.7 Hz, 2H), 4.06 (s, 3H), 3.29–3.20 (m, 2H), 2.87–2.77 (m, 2H), 1.93–1.82 (m, 2H), 1.65–1.52 (m, 2H), 1.48–1.39 (m, 2H), 1.34–1.29 (m, 2H), 1.23 (br s, 6H). ¹³C NMR (400 MHz, DMSO-*d*₆) δ 158.9–158.6 (m, 2C), 150.8 (s, 1C), 150.4–149.8 (m, 1C), 149.0 (s, 2C), 147.7 (s, 1C), 145.3 (s, 1C), 142.9 (s, 1C), 137.9–137.5 (s, 2C), 130.6 (s, 1C), 126.7 (s, 1C), 125.0 (s, 1C), 124.1 (s, 1C), 123.3 (s, 1C), 121.7 (s, 1C), 120.4 (s, 1C), 120.2 (s, 1C), 117.4 (s, 1C), 114.5 (s, 1C), 108.4 (s, 1C), 105.4 (s, 1C), 102.1 (s, 1C), 74.3 (s, 1C), 57.0–56.8 (m, 3C), 55.3 (s, 1C), 53.9 (s, 1C), 29.5 (s, 1C), 28.7–28.4 (m, 2C), 26.4 (s, 1C), 25.9 (s, 1C), 25.2 (s, 1C), 23.2 (s, 1C). ESI-MS *m/z*: 645.3 [M – (TFA-H)]⁺ (Tris-HCl buffer solution containing 5% DMSO as solvent). Elemental analysis calcd (%) for C₄₂H₄₅F₃N₄O₆: C 66.48, H 5.98, and N 7.38; found: C 66.45, H 6.00, and N 7.36. ¹⁹F NMR (471 MHz, CHCl₃) δ –75.8.

General procedure for preparation of compound 8. Jatrorrhizine (**7**) (0.500 g, 1.33 mmol, 1.00 eq., HCl) and compound **3** (954 mg, 3.33 mmol, 2.50 eq.) were dissolved in MeCN (15.0 mL), K₂CO₃ (553 mg, 4.00 mmol, 3.00 eq.) was added to mixture at 25 °C, then warmed to 60 °C for 16 h, TLC (dichloromethane : methanol = 5 : 1, R_f = 0.54) indicated compound **7** (0.500 g, 1.33 mmol, 1.00 eq., HCl) was consumed completely and many new spots formed. The reaction of 6 batches were used directly in the next step without work-up. The reaction of 6 batches were used directly in the next step without purification. The reaction of 6 batches were used directly in the next step. ESI-MS *m/z*: 542.2 [M – Cl]⁺ (Tris-HCl buffer solution containing 5% DMSO as solvent). Elemental analysis calcd (%) for C₂₉H₃₇BrClNO₄: C 60.16, H 6.44, and N 2.42; found: C 60.15, H 6.46, and N 2.40.

General procedure for preparation of J-TFA. A mixture of compound **8** (0.750 g, 1.29 mmol, 1.00 eq., HCl) and compound **5** (515 mg, 2.59 mmol, 2.50 eq.) and KI (172 mg, 1.03 mmol, 0.800 eq.) were dissolved in MeCN (6.00 mL) at 25 °C and warmed at 90 °C for 4 h. The mixture of 6 batches were together filtered to obtain the filtrate. The filtrate was evaporated to obtain the crude product. Consequently, these crude product was purified by reversed-phase HPLC (column: Welch Xtimate C18 250 × 50 mm × 10 μm; mobile phase: [water (0.1%TFA)-ACN]; B%: 10%–40%, 20 min). LC-MS and ¹H NMR compound *N,N*-bis(2-pyridylmethyl)-9-[(2,9,10-trimethoxy-5,6-dihydroisoquinolino[3,2-*a*]isoquinolin-7-ium-3-yl)

oxy]nonan-1-amine (**J-TFA**) (1.20 g, 1.47 mmol, 18.9% yield) was obtained as a yellow oil. ^1H NMR (400 MHz, $\text{CH}_3\text{OH}-d_4$): δ = 9.78 (s, 1H), 8.82 (s, 1H), 8.69 (d, J = 4.8 Hz, 2H), 8.18–8.12 (m, 1H), 8.03 (d, J = 9.1 Hz, 1H), 7.93 (dt, J = 1.6, 7.7 Hz, 2H), 7.69 (s, 1H), 7.53 (d, J = 7.8 Hz, 2H), 7.48 (dd, J = 5.2, 7.3 Hz, 2H), 7.05 (s, 1H), 4.95 (br t, J = 6.3 Hz, 2H), 4.63 (s, 4H), 4.23 (s, 3H), 4.15–4.09 (m, 5H), 4.02 (s, 3H), 3.33 (br s, 2H), 3.29 (s, 2H), 1.92–1.81 (m, 4H), 1.59–1.49 (m, 2H), 1.38 (br s, 8H). ESI-MS m/z : 660.9 $[\text{M} - (\text{TFA}-\text{H})]^+$ (Tris-HCl buffer solution containing 5% DMSO as solvent). Elemental analysis calcd (%) for $\text{C}_{43}\text{H}_{49}\text{F}_3\text{N}_4\text{O}_6$: C 66.65, H 6.37, and N 7.23; found: C 66.62, H 6.39, and N 7.22. ^{19}F NMR (471 MHz, CH_3OH) δ -77.3.

Synthesis and characterization of Pt1 and Pt2

The *cis*-Pt(DMSO) $_2$ Cl $_2$ (1.0 mmol) was mixed with 1.0 mmol **B-TFA** and **J-TFA** in CH_3CN (5.0 mL) at 60 °C for 4.0 h to yield yellow product of **Pt1** and **Pt2**, which were isolated and characterized (Fig. 1).

Data for Pt1. Yield: 87.06%. ESI-MS: m/z = 987.4 for $[\text{M} - \text{Cl}]^+$ (Tris-HCl buffer solution containing 5% DMSO as solvent), m/z = 914.2 for $[\text{M} - (\text{TFA}-\text{H})]^+$. Elemental analysis: calcd (%) for $\text{C}_{42}\text{H}_{45}\text{Cl}_2\text{F}_3\text{N}_4\text{O}_6\text{Pt}$: C 49.22, H 4.43, N 5.47; found: C 49.20 H 4.46, N 5.44. ^1H NMR (500 MHz, $\text{DMSO}-d_6$) δ 9.72 (s, 1H), 8.92 (s, 1H), 8.77 (d, J = 5.3 Hz, 2H), 8.31 (t, J = 7.2 Hz, 2H), 8.23–8.09 (m, 1H), 7.99 (s, 1H), 7.85 (s, 2H), 7.75 (s, 1H), 7.67 (t, J = 6.6 Hz, 2H), 7.08 (s, 1H), 6.18 (s, 2H), 5.37 (s, 2H), 4.94 (d, J = 31.1 Hz, 4H), 4.24 (t, J = 6.4 Hz, 2H), 4.04 (s, 3H), 3.05 (s, 2H), 2.52 (s, 2H), 1.90–1.75 (m, 2H), 1.51 (s, 2H), 1.40 (t, J = 7.9 Hz, 2H), 1.31–1.20 (m, 4H), 1.16 (d, J = 14.4 Hz, 4H). ^{13}C NMR (126 MHz, $\text{DMSO}-d_6$) δ 166.3, 158.4, 158.2, 150.8, 150.2, 149.4, 148.1, 145.7, 143.3, 141.8, 137.9, 133.4, 131.1, 127.1, 125.9, 124.0, 123.8, 122.1, 120.9, 120.7, 108.9, 105.9, 102.6, 74.7, 68.5, 64.8, 57.5, 55.8, 40.6, 40.4, 40.2, 40.1, 39.9, 39.7, 39.6, 29.9, 29.3, 29.1, 29.0, 27.6, 26.9, 26.3, 25.6. ^{19}F NMR (471 MHz, $\text{DMSO}-d_6$) δ -73.5. Elemental analysis calcd (%) for $\text{C}_{42}\text{H}_{45}\text{Cl}_2\text{F}_3\text{N}_4\text{O}_6\text{Pt}$: C 49.22, H 4.43, and N 5.47; found: C 49.20, H 4.46, and N 5.45.

Data for Pt2. Yield: 95.66%. ESI-MS: m/z = 928.0 for $[\text{M} - (\text{TFA}-\text{H})]^+$, m/z = 1002.8 for $[\text{M} - \text{Cl}]^+$. Elemental analysis: calcd (%) for $\text{C}_{43}\text{H}_{49}\text{Cl}_2\text{F}_3\text{N}_4\text{O}_6\text{Pt}$: C 49.62, H 4.75, N 5.38; found: C 49.60, H 4.78, N 5.36. ^1H NMR (500 MHz, $\text{DMSO}-d_6$) δ 9.89 (s, 1H), 9.05 (s, 1H), 8.80–8.76 (m, 2H), 8.30 (td, J = 7.8, 1.6 Hz, 2H), 8.19 (d, J = 9.2 Hz, 1H), 8.05 (d, J = 9.1 Hz, 1H), 7.83 (d, J = 7.9 Hz, 2H), 7.69 (s, 1H), 7.68–7.65 (m, 2H), 7.05 (s, 1H), 5.36 (d, J = 15.9 Hz, 2H), 4.97 (t, J = 6.3 Hz, 2H), 4.87 (d, J = 15.8 Hz, 2H), 4.11 (s, 3H), 4.07 (s, 3H), 4.02 (t, J = 6.6 Hz, 2H), 3.94 (s, 3H), 3.23 (t, J = 6.4 Hz, 2H), 3.06–2.99 (m, 2H), 1.69 (p, J = 6.8 Hz, 2H), 1.49 (td, J = 11.3, 9.6, 5.9 Hz, 2H), 1.34 (t, J = 7.8 Hz, 2H), 1.25–1.19 (m, 4H), 1.12 (dt, J = 13.4, 7.2 Hz, 4H). ^{13}C NMR (126 MHz, $\text{DMSO}-d_6$) δ 166.3, 161.7, 158.9, 158.6, 158.4, 158.1, 151.3, 150.6, 149.5, 149.2, 145.9, 144.0, 141.8, 138.2, 133.6, 129.0, 127.2, 125.8, 123.9, 123.9, 121.8, 120.9, 120.3, 119.2, 118.5, 116.1, 113.8, 112.5, 109.3, 68.9, 68.4, 64.7, 62.4, 57.5, 56.6, 55.9, 40.5, 40.4, 40.2, 40.0, 39.8, 39.7, 39.5, 29.0, 28.9, 28.8, 28.7, 27.5, 26.4, 26.2, 25.8. ^{19}F NMR (471 MHz, $\text{DMSO}-d_6$) δ -73.9. Elemental analysis calcd (%) for

$\text{C}_{43}\text{H}_{49}\text{Cl}_2\text{F}_3\text{N}_4\text{O}_6\text{Pt}$: C 49.62, H 4.75, and N 5.38; found: C 49.59, H 4.77, and N 5.36.

Materials and methods

For materials, the detailed methods and procedures of **B-TFA**, **TFA**, **J-TFA**, their **Pt1** and **Pt2** complexes see in ESI.†

Conclusions

In summary, two novel Pt(II) complexes **Pt1** and **Pt2** with jatrorrhizine and berberine derivatives were prepared. Their green-colored luminescent properties and potent telomerase inhibition were explored. *In vitro* and *in vivo* cytotoxicity results suggested that human bladder T-24 tumor cells were sensitive to **Pt1** and **Pt2**. These two novel Pt(II) complexes induced cancer cell apoptosis *via* targeting telomerase, together with inducing mitochondrial dysfunction, damaging telomere DNA and arresting cell-cycle. Remarkably, the *in vivo* results illustrated that jatrorrhizine **Pt2** complex exhibited high safety and even more effective inhibitory effect (TIR = 50.4%) on T-24 tumor xenograft than berberine **Pt1** complex (26.4%) and cisplatin (37.1%). Therefore, jatrorrhizine **Pt2** complex may have the potential to be further developed into safe and effective Pt-based anticancer agents.

Conflicts of interest

There are no conflicts to declare.

Acknowledgements

This work is supported by the National Natural Science Foundation of China (No. 21867017, 21761033 and 21565028), the Natural Science Foundation of Guangxi (No. 2018GXNSFBA138021 and 2018GXNSFBA281188) as well as the Innovative Team & Outstanding Talent Program of Colleges and Universities in Guangxi (2014-49 and 2017-38).

The animal procedures were approved by the Institute of Radiation Medicine Chinese Academy of Medical Sciences (Tian Jin, China, approval No. SYXK 2014-0002). And all of the experimental procedures were carried out in accordance with the NIH Guidelines for the Care and Use of Laboratory Animals. Animal experiments were approved by the Animal Care and Use Committee of Institute of Radiation Medicine Chinese Academy of Medical Sciences.

Notes and references

- (a) L. Kelland, *Nat. Rev. Cancer*, 2007, 7, 573–584;
(b) R. R. Vernooij, T. Joshi, M. D. Horbury, B. Graham, E. I. Izgorodina, V. G. Stavros, P. J. Sadler, L. Spiccia and

- B. R. Wood, *Chem. – Eur. J.*, 2018, **24**, 5790–5803; (c) C. Ouyang, L. Chen, T. W. Rees, Y. Chen, J. Liu, L.-N. Ji, J. Long and H. Chao, *Chem. Commun.*, 2018, **54**, 6268–6271; (d) I. Romero-Canelón, L. Salassa and P. J. Sadler, *J. Med. Chem.*, 2013, **56**, 1291–1300; (e) Y. Gothe, T. Marzo, L. Messori and N. Metzler-Nolte, *Chem. – Eur. J.*, 2016, **22**, 12487–12494; (f) M. Patra, G. Gasser and N. Metzler-Nolte, *Dalton Trans.*, 2012, **41**, 6350–6358.
- 2 (a) A. De Cian, G. Cristofari, P. Reichenbach, E. De Lemos, D. Monchaud, M.-P. Teulade-Fichou, K. Shin-ya, L. Lacroix, J. Lingner and J.-L. Mergny, *Proc. Natl. Acad. Sci. U. S. A.*, 2007, **104**, 17347–17352; (b) T. T.-H. Fong, C.-N. Lok, C. Y.-S. Chung, Y.-M. E. Fung, P.-K. Chow, P.-K. Wan and C.-M. Che, *Angew. Chem., Int. Ed.*, 2016, **55**, 11935–11939.
- 3 (a) Z. Xue, M. Lin, J. Zhu, J. Zhang, Y. Li and Z. Guo, *Chem. Commun.*, 2010, **46**, 1212–1214; (b) M. Galanski, S. Slaby, M. A. Jakupec and B. K. Keppler, *J. Med. Chem.*, 2003, **46**, 4946–4951; (c) N. Margiotta, R. Ostuni, D. Teoli, M. Morpurgo, N. Realdon, B. Palazzo and G. Natile, *Dalton Trans.*, 2007, 3131–3139.
- 4 (a) R. Sasanelli, A. Boccarelli, D. Giordano, M. Laforgia, F. Arnesano, G. Natile, C. Cardellicchio, M. A. Capozzi and M. Coluccia, *J. Med. Chem.*, 2007, **50**, 3434–3441; (b) R. N. Bose, L. Maurmann, R. J. Mishur, L. Yasui, S. Gupta, W. S. Grayburn, H. Hofstetter and T. Salley, *Proc. Natl. Acad. Sci. U. S. A.*, 2008, **105**, 18314–18319; (c) Y.-R. Zheng, K. Suntharalingam, T. C. Johnstone and S. J. Lippard, *Chem. Sci.*, 2015, **6**, 1189–1193; (d) S. P. Wisnovsky, J. J. Wilson, R. J. Radford, M. P. Pereira, M. R. Chan, R. R. Laposa, S. J. Lippard and S. O. Kelley, *Chem. Biol.*, 2013, **20**, 1323–1328; (e) V. T. Yilmaz, C. Icsel, O. R. Turgut, M. Aygun, M. Erkisa, M. H. Turkdemir and E. Ulukaya, *Eur. J. Med. Chem.*, 2018, **155**, 609–622; (f) L. Fang, X. Qin, J. Zhao and S. Gou, *Inorg. Chem.*, 2019, **58**, 2191–2200; (g) X.-H. Zheng, G. Mu, Y.-F. Zhong, T.-P. Zhang, Q. Cao, L.-N. Ji, Y. Zhao and Z.-W. Mao, *Chem. Commun.*, 2016, **52**, 14101–14104.
- 5 (a) K. K. W. To, S. C. F. Au-Yeung and Y.-P. Ho, *Anti-Cancer Drugs*, 2006, **17**, 673–683; (b) Y.-P. Ho, K. K. W. To, S. C. F. Au-Yeung, X. Wang, G. Lin and X. Han, *J. Med. Chem.*, 2001, **44**, 2065–2068; (c) H. D. Zinsmeister, H. Becker and T. Eicher, *Angew. Chem., Int. Ed. Engl.*, 1991, **30**, 130–147; (d) Z.-F. Chen, Y.-C. Liu, K.-B. Huang and H. Liang, *Curr. Top. Med. Chem.*, 2013, **13**, 2104–2115.
- 6 (a) Z.-F. Chen, Y.-F. Shi, Y.-C. Liu, X. Hong, B. Geng, Y. Peng and H. Liang, *Inorg. Chem.*, 2012, **51**, 1998–2009; (b) Z.-F. Chen, Y.-C. Liu, L.-M. Liu, H.-S. Wang, S.-H. Qin, B.-L. Wang, H.-D. Bian, B. Yang, H.-K. Fun, H.-G. Liu, H. Liang and C. Orvig, *Dalton Trans.*, 2009, 262–272; (c) Y.-C. Liu, Z.-F. Chen, L.-M. Liu, Y. Peng, X. Hong, B. Yang, H.-G. Liu, H. Liang and C. Orvig, *Dalton Trans.*, 2009, 10813–10823; (d) Z.-F. Chen, M.-X. Tan, L.-M. Liu, Y.-C. Liu, H.-S. Wang, B. Yang, Y. Peng, H.-G. Liu, H. Liang and C. Orvig, *Dalton Trans.*, 2009, 10824–10833.
- 7 (a) Z.-F. Chen, Q.-P. Qin, J.-L. Qin, Y.-C. Liu, K.-B. Huang, Y.-L. Li, T. Meng, G.-H. Zhang, Y. Peng, X.-J. Luo and H. Liang, *J. Med. Chem.*, 2015, **58**, 2159–2179; (b) Z.-F. Chen, Q.-P. Qin, J.-L. Qin, J. Zhou, Y.-L. Li, N. Li, Y.-C. Liu and H. Liang, *J. Med. Chem.*, 2015, **58**, 4771–4789; (c) Q.-P. Qin, Z.-F. Wang, X.-L. Huang, M.-X. Tan, B.-B. Shi and H. Liang, *ACS Med. Chem. Lett.*, 2019, **10**, 936–940.
- 8 T. Tauchi, K. Shin-ya, G. Sashida, M. Sumi, S. Okabe, J. H. Ohyashiki and K. Ohyashiki, *Oncogene*, 2006, **25**, 5719–5725.
- 9 (a) J. Li, J. Li, Y. Jiao and C. Dong, *Spectrochim. Acta, Part A*, 2014, **118**, 48–54; (b) Y. C. Deng, M. Zhang and H. Y. Luo, *Ind. Crops Prod.*, 2012, **37**, 298–302; (c) R. Liu, Z. Cao, Y. Pan, G. Zhang, P. Yang, P. Guo and Q. Zhou, *Anti-Cancer Drugs*, 2013, **24**, 667–676; (d) W. Kong, J. Wei, P. Abidi, M. Lin, S. Inaba, C. Li, Y. Wang, Z. Wang, S. Si, H. Pan, S. Wang, J. Wu, Y. Wang, Z. Li, J. Liu and J.-D. Jiang, *Nat. Med.*, 2004, **10**, 1344–1351; (e) Y. Ma, T.-M. Ou, J.-Q. Hou, Y.-J. Lu, J.-H. Tan, L.-Q. Gu and Z.-S. Huang, *Bioorg. Med. Chem.*, 2008, **16**, 7582–7591; (f) H. Jiang, X. Wang, L. Huang, Z. Luo, T. Su, K. Ding and X. Li, *Bioorg. Med. Chem.*, 2011, **19**, 7228–7235; (g) Y. Wang, W. Pang, Q. Zeng, Z. Deng, T. Fan, J. Jiang, H. Deng and D. Song, *Eur. J. Med. Chem.*, 2018, **143**, 1858–1868.
- 10 (a) Q.-P. Qin, J.-L. Qin, T. Meng, W.-H. Lin, C.-H. Zhang, Z.-Z. Wei, J.-N. Chen, Y.-C. Liu, H. Liang and Z.-F. Chen, *Eur. J. Med. Chem.*, 2016, **124**, 380–392; (b) T. Billaud, C. Brun, K. Ancelin, C. E. Koering, T. Laroche and E. Gilson, *Nat. Genet.*, 1997, **17**, 236–239; (c) A. Smogorzewska, B. van Steensel, A. Bianchi, S. Oelmann, M. R. Schaefer, G. Schnapp and T. de Lange, *Mol. Cell Biol.*, 2000, **20**, 1659–1668; (d) G. B. Celli and T. de Lange, *Nat. Cell Biol.*, 2005, **7**, 712–718; (e) A. Fradet-Turcotte, M. D. Canny, C. Escribano-Díaz, A. Orthwein, C. C. Y. Leung, H. Huang, M.-C. Landry, J. Kitevski-LeBlanc, S. M. Noordermeer, F. Sicheri and D. Durocher, *Nature*, 2013, **499**, 50–54.
- 11 (a) J.-Q. Hou, S.-B. Chen, L.-P. Zan, T.-M. Ou, J.-H. Tan, L. G. Luyt and Z.-S. Huang, *Chem. Commun.*, 2015, **51**, 198–201; (b) Y. Zhao, D. Cheng, S. Wang and J. Zhu, *Nucleic Acids Res.*, 2014, **42**, 10385–10398; (c) M. Chalfie, Y. Tu, G. Euskirchen, W. W. Ward and D. C. Prasher, *Science*, 1994, **263**, 802–805; (d) T.-C. He, A. B. Sparks, C. Rago, H. Hermeking, L. Zawel, L. T. da Costa, P. J. Morin, B. Vogelstein and K. W. Kinzler, *Science*, 1998, **281**, 1509–1512; (e) D. Monchaud, C. Allain, H. Bertrand, N. Smargiasso, F. Rosu, V. Gabelica, A. De Cian, J.-L. Mergny and M.-P. Teulade-Fichou, *Biochimie*, 2008, **90**, 1207–1223; (f) V. S. Stafford, K. Suntharalingam, A. Shivalingam, A. J. P. White, D. J. Mann and R. Vilar, *Dalton Trans.*, 2015, **44**, 3686–3700; (g) O. Domarco, D. Lötsch, J. Schreiber, C. Dinhof, S. Van Schoonhoven, M. D. García, C. Peinador, B. K. Keppler, W. Berger and A. Terenzi, *Dalton Trans.*, 2017, **46**, 329–332; (h) A. De Cian, E. DeLemos, J.-L. Mergny, M.-P. Teulade-Fichou and D. Monchaud, *J. Am. Chem. Soc.*, 2007, **129**, 1856–1857.

- 12 (a) A. K. P. Taggart, S.-C. Tenga and V. A. Zakian, *Science*, 2002, **297**, 1023–1026; (b) Q.-P. Qin, Z.-F. Wang, S.-L. Wang, D.-M. Luo, B.-Q. Zou, P.-F. Yao, M.-X. Tan and H. Liang, *Eur. J. Med. Chem.*, 2019, **170**, 195–202.
- 13 (a) A. Kyziol, A. Cierniak, J. Gubernator, A. Markowski, M. Jezowska-Bojczuk and U. K. Komarnicka, *Dalton Trans.*, 2018, **47**, 1981–1992; (b) Q.-P. Qin, S.-L. Wang, M.-X. Tan, Z.-F. Wang, X.-L. Huang, Q.-M. Wei, B.-B. Shi, B.-Q. Zou and H. Liang, *Metallomics*, 2018, **10**, 1160–1169; (c) M. B. Kastan and J. Bartek, *Nature*, 2004, **432**, 316–323; (d) Q.-P. Qin, S.-L. Wang, M.-X. Tan, Z.-F. Wang, D.-M. Luo, B.-Q. Zou, Y.-C. Liu, P.-F. Yao and H. Liang, *Eur. J. Med. Chem.*, 2018, **158**, 106–122; (e) T. Meng, Q.-P. Qin, Z.-L. Chen, H.-H. Zou, K. Wang and F.-P. Liang, *Dalton Trans.*, 2019, **48**, 5352–5360; (f) Q.-P. Qin, Z.-F. Wang, M.-X. Tan, X.-L. Huang, H.-H. Zou, B.-Q. Zou, B.-B. Shi and S.-H. Zhang, *Metallomics*, 2019, **11**, 1005–1015.
- 14 (a) S. Göschl, E. Schreiber-Brynzak, V. Pichler, K. Cseh, P. Heffeter, U. Jungwirth, M. A. Jakupec, W. Berger and B. K. Keppler, *Metallomics*, 2017, **9**, 309–322; (b) A. Weiss, R. H. Berndsen, M. Dubois, C. Muller, R. Schibli, A. W. Griffioen, P. J. Dyson and P. Nowak-Sliwinska, *Chem. Sci.*, 2014, **5**, 4742–4748.
- 15 (a) Y. Wang, J. Xiao, H. Zhou, S. Yang, X. Wu, C. Jiang, Y. Zhao, D. Liang, X. Li and G. Liang, *J. Med. Chem.*, 2011, **54**, 3768–3778; (b) J.-Q. Wang, P.-Y. Zhang, L.-N. Ji and H. Chao, *J. Inorg. Biochem.*, 2015, **146**, 89–96; (c) L. Xu, X. Chen, J. Wu, J. Wang, L. Ji and H. Chao, *Chem. – Eur. J.*, 2015, **21**, 4008–4020; (d) L. Zeng, P. Gupta, Y. Chen, E. Wang, L. Ji, H. Chao and Z.-S. Chen, *Chem. Soc. Rev.*, 2017, **46**, 5771–5804.